Published OnlineFirst December 19, 2017; DOI: 10.1158/1078-0432.CCR-17-1795

Personalized Medicine and Imaging

Clinical Cancer Research

Optical Analysis of Glioma: Fourier-Transform Infrared Spectroscopy Reveals the *IDH1* Mutation Status

Ortrud Uckermann[1,2], Tareq A. Juratli[1], Roberta Galli[3], Marina Conde[1], Ralf Wiedemuth[1], Dietmar Krex[1,2], Kathrin Geiger[4], Achim Temme[1,2], Gabriele Schackert[1,2], Edmund Koch[3,5], Gerald Steiner[3], and Matthias Kirsch[1,2,5]

Abstract

Purpose: Somatic mutations in the human cytosolic isocitrate dehydrogenase 1 (*IDH1*) gene cause profound changes in cell metabolism and are a common feature of gliomas with unprecedented predictive and prognostic impact. Fourier-transform infrared (FT-IR) spectroscopy addresses the molecular composition of cells and tissue and was investigated to deduct the *IDH1* mutation status.

Experimental Design: We tested the technique on human cell lines that were transduced with wild-type *IDH1* or mutated *IDH1* and on 34 human glioma samples. IR spectra were acquired at 256 positions from cell pellets or tissue cryosections. Moreover, IR spectra were obtained from fresh, unprocessed biopsies of 64 patients with glioma.

Results: *IDH1* mutation was linked to changes in spectral bands assigned to molecular groups of lipids and proteins in cell lines and human glioma. The spectra of cryosections of brain tumor samples showed high interpatient variability, for example, bands related to calcifications at 1113 cm^{-1}. However, supervised classification recognized relevant spectral regions at 1103, 1362, 1441, 1485, and 1553 cm^{-1} and assigned 88% of the tumor samples to the correct group. Similar spectral positions allowed the classification of spectra of fresh biopsies with an accuracy of 86%.

Conclusions: Here, we show that vibrational spectroscopy reveals the *IDH1* genotype of glioma. Because it can provide information in seconds, an implementation into the intraoperative workflow might allow simple and rapid online diagnosis of the *IDH1* genotype. The intraoperative confirmation of *IDH1* mutation status might guide the decision to pursue definitive neurosurgical resection and guide future *in situ* therapies of infiltrative gliomas. *Clin Cancer Res; 24(11); 2530–8.* ©2017 AACR.

See related commentary by Hollon and Orringer, p. 2467

Introduction

Somatic mutations of the isocitrate dehydrogenase 1 and 2 (*IDH1* and *IDH2*) genes are frequent and early causative events in the pathogenesis of a subset of gliomas, mainly low-grade gliomas and secondary glioblastomas (1–3). Patients with *IDH*-mutated tumors show improved survival compared with patients who have *IDH* wild-type gliomas of the same histologic grade (4). Hence, it became increasingly apparent that *IDH* mutation status accounts for much of the prognostic information previously rendered by histologic grading (5). The latter fact underscores the prognostic significance and the clinical impact of *IDH* mutations in patients with glioma.

IDH mutations inactivate the standard enzymatic activity and confer novel activity on IDH1 for conversion of α-ketoglutarate to 2-hydroxyglutarate (2HG). This gain of function causes an accumulation in glioma cells of 2HG (6), an oncometabolite that drives the oncogenic activity of *IDH* mutations contributing to malignant transformation and glioma genesis through several pathways (7). *IDH* mutations and/or 2HG accumulation represent ideal surrogate markers for both diagnosis and for monitoring the treatment response in affected tumors.

As testing for *IDH1/2* mutations is now considered standard by international guidelines for glioma management, reliable and effective methods of detection are of paramount importance (8). *IDH* mutation detection methods include IHC, DNA sequencing, and PCR analysis, all of which rely on invasive tissue or cerebrospinal fluid sampling for mutation detection (9). One important limitation is that all these methods involve long analytic times, which take several days and expensive equipment, making a rapid diagnosis unlikely. In addition, several methods have been reported to test for the presence of 2HG in tumor samples (6)

[1]Neurosurgery, University Hospital Carl Gustav Carus, Technische Universität (TU) Dresden, Dresden, Germany. [2]German Cancer Consortium (DKTK) Dresden, National Center for Tumor Diseases (NCT), Partner Site Dresden, Dresden, Germany. [3]Clinical Sensoring and Monitoring, Department of Anesthesiology and Intensive Care Medicine, Faculty of Medicine, TU Dresden, Dresden, Germany. [4]Neuropathology, University Hospital Carl Gustav Carus, TU Dresden, Dresden, Germany. [5]CRTD/DFG-Center for Regenerative Therapies Dresden - Cluster of Excellence, Dresden, Germany.

Note: Supplementary data for this article are available at Clinical Cancer Research Online (http://clincancerres.aacrjournals.org/).

O. Uckermann and T.A. Juratli contributed equally to this article.

O. Uckermann and T.A. Juratli share first authorship

Corresponding Authors: Matthias Kirsch, University Hospital Carl Gustav Carus, TU Dresden, Faculty of Medicine, Fetscherstr. 74, Dresden 01307, Germany. Phone: 4935-1458-4735; Fax: 4935-1458-4304; E-mail: Matthias.kirsch@uniklinikum-dresden.de; and Gerald Steiner, Clinical Sensoring and Monitoring, Department of Anesthesiology and Intensive Care Medicine, Faculty of Medicine, TU Dresden, Fetscherstr. 74, Dresden 01307, Germany. Phone: 4935-1458-6618, Fax: 4935-1458-6325; E-mail: Gerald.steiner@tu-dresden.de

doi: 10.1158/1078-0432.CCR-17-1795

Published OnlineFirst December 19, 2017; DOI: 10.1158/1078-0432.CCR-17-1795

Translational Relevance

Patients with *IDH1*-mutated tumors show superior survival compared with patients who have *IDH1* wild-type gliomas of the same histologic grade. Furthermore, the determination of the *IDH1* genotype is essential for current glioma grading according to the World Health Organization (WHO). Here, we show that vibrational spectroscopy, a technology that can provide intraoperative diagnostic information in seconds, can reveal the *IDH1* mutation status of human glioma samples. The development of a simple and rapid diagnostic technique for *IDH1* is of paramount importance, because conclusive intraoperative confirmation of *IDH1* mutation status might guide the decision to pursue definitive neurosurgical resection and guide future *in situ* therapies of diffuse infiltrative gliomas. Besides *IDH1*, other diagnostic, prognostic, and predictive molecular markers of tumors might be amenable to vibrational spectroscopy and, therefore, to fast and label-free intraoperative profiling.

as well as noninvasively using magnetic resonance spectroscopic technology (10, 11). Quantitatively measuring 2HG in tumor cells over time may assist in monitoring for tumor recurrence, differentiate treatment effect from pseudoprogression, and assess tumor response to *IDH*-specific pharmacotherapies (12). However, no intraoperative 2HG detection method with a high accuracy has been described to date. Along this line of thinking, conclusive intraoperative confirmation of *IDH* mutations might guide the decision to pursue definitive neurosurgical resection in diffuse infiltrative glioma (13) or pave the way to *IDH1*-dependent *in situ* therapeutics and therapy.

"Vibrational spectroscopy" is the collective term used to describe two analytic techniques: infrared and Raman spectroscopy. They probe vibrational energy levels that are associated with the chemical bonds in the sample without the need for labeling. Both are nondestructive, noninvasive tools that deliver comprehensive information about the sample's composition in the form of a spectrum. Several reports highlighted the potential of vibrational spectroscopy for clinical applications (14–16). Moreover, intraoperative detection (17) and diagnosis (18) of glioma were recently reported. By using these techniques, it is possible to distinguish brain tissue from necrosis and tumor (19), to provide tumor type and grade (20), to identify the origin of brain metastases (21), and to discriminate tumors that differ in a single molecular alteration, such as hormone-producing and hormone-inactive pituitary adenoma (22).

The development of a simple, rapid, specific, and sensitive diagnostic technique for *IDH* mutations based on vibrational spectroscopy might provide valuable intraoperative diagnosis in affected patients. Therefore, we investigated the ability of Fourier-transform infrared (FT-IR) spectroscopy to analyze the *IDH1* mutation status in glioma samples.

Materials and Methods

Cell lines

The near tetraploid primary glioblastoma cell line HT7606 has been described recently (23). The immortalized astrocytoma cell lines SVGp12 and U87-MG were authenticated using SNP profiling (Multiplexion GmbH) and cultured in Basal Minimal Eagle medium (catalog no. 41010-026) supplemented with 10% v/v heat-inactivated FBS (catalog no. A15-101), 2 mmol/L L-glutamine (catalog no. 25030-024), and 1% nonessential amino acids (catalog no. M11-003; all from Gibco). All cell lines were tested as free of *Mycoplasma* contamination using MycoAlert kit (Lonza Cologne GmbH).

cDNAs, lentiviral vectors, and transduction of cells

The coding regions of human IDH1 and IDHR^{132H} fused to a C-terminal His6- and myc-tags and flanked by AgeI and NotI restriction were synthesized (Eurofins MWG Biotech) and ligated into AgeI/NotI-digested lentiviral vector pHATtrick-puro (24). All vectors were confirmed by DNA sequencing. Lentiviral particle production and transduction of cells were performed as described previously (24).

Human brain tumors and IDH1 mutation determination

Human brain tumor tissue was obtained during routine tumor surgery. The patients gave written consent; the study was approved by the ethics committee at the University Hospital Carl Gustav Carus, Technische Universität Dresden (Dresden, Germany; EK 323122008); and the study was conducted in accordance with the Declaration of Helsinki. A total of 98 tumor samples from 90 patients with glioma were analyzed (Supplementary Tables S1 and S2). The samples were either directly subjected to attenuated total reflection (ATR) FT-IR without any processing or snap frozen at −80 °C and embedded in tissue freezing medium (catalog no. 14020108926; Leica Microsystems) to prepare cryosections of 16-μm thickness on glass or CaF_2 slides for FT-IR spectroscopy.

After ATR FT-IR, the samples were formalin fixed and subjected to diagnostic histopathologic workup. *IDH1* mutations were assessed using direct DNA sequencing, as reported elsewhere (2) or by standard IDH1 IHC.

Transmission FT-IR spectroscopic imaging

IR spectra were acquired in transmission from dry cell pellet preparations on CaF_2 slides ($n = 3$ replicates for each group) or unstained cryosections of human brain tumors ($n = 34$). The area of measurement in the human brain tumor samples was chosen according to the evaluation of stained consecutive sections by a pathologist.

The system used was described elsewhere (25). Briefly, IR spectra were acquired in transmission mode with an FT-IR spectrometer TENSOR 27 equipped with an IR microscope HYPERION 3000 (both from Bruker Optics GmbH) and a 15× Cassegrain objective (0.4 NA). An area of 175 μm × 175 μm was imaged by a 64 × 64 mercury cadmium telluride focal-plane array detector using a spectral resolution of 6 cm^{-1}. A background spectrum was recorded from pure CaF_2 slide. A total of 200 interferograms were coadded and Fourier transformed by applying Blackman–Harris apodization without filling. Each transmission spectrum was ratioed to the background spectrum. The transmission spectra were converted to absorbance values. For each sample (both cells and tumor cryosections), a single area was imaged, and thus, 4096 spectra were acquired in approximately 1 minute.

An atmospheric compensation was performed to subtract contributions of residual water vapor bands from the spectra and 4 × 4 binning was applied in OPUS 7.2 (Bruker Optics GmbH).

Published OnlineFirst December 19, 2017; DOI: 10.1158/1078-0432.CCR-17-1795

ATR FT-IR spectroscopy

ATR IR spectra were acquired from 64 fresh, unprocessed tumor biopsies. The system used was described elsewhere (26). Briefly, measurements were performed on a portable ALPHA-P ATR spectrometer (Bruker Optics GmbH) equipped with a diamond crystal. The instrument's anvil was used to force the contact between crystal and sample. Measurements were performed using a spectral resolution of 4 cm^{-1} and coadding of 128 interferograms and Fourier transformed by applying Blackman–Harris apodization without filling. Spectra were ratioed against the background spectrum that was recorded without sample. One spectrum was obtained for each sample, and the measurement time was approximately 1 minute.

Spectroscopic data analyses and classification

Further analysis was performed using the MATLAB package (MathWorks Inc.). Data were reduced to the spectral region of 950 to 1800 cm^{-1}. A linear baseline was applied, followed by normalization.

The differentiation of cell lines expressing wild-type *IDH1* (*IDH1*-wt) or mutated *IDH1* (*IDH1*-mut) was obtained using a classification by quadratic discriminant analysis (function classify in MATLAB) combined with manual feature selection based on the comparison with the 2HG reference spectrum and the difference spectrum of *IDH1*-mut versus *IDH1*-wt cell lines. The training set consisted of 25% of the dataset (1728 spectra).

The classification function for human brain tumors was developed and tested using spectra of 34 cryosections. The algorithm was implemented in MATLAB as described elsewhere (27). The spectra of four *IDH1*-wt samples and four *IDH1*-mut samples were selected by the algorithm and used as training set. An optimal selection routine was applied on the training set to retrieve the spectral regions that contained the information discriminating *IDH1*-wt and *IDH1*-mut. The performance of the classification was assessed with the leave-one-out cross-validation method. After optimization of the classification rate on the training data, the remaining spectra served as an independent test set and were analyzed using those selected spectral regions and quadratic discriminant analysis.

Spectra of fresh brain tumor biopsies ($n = 64$) were classified using quadratic discriminant analysis based on spectral regions selected by the algorithm described above in combination with manual feature selection using the regions identified on glioma cryosections. Ten spectra of *IDH1*-wt samples and 10 spectra of *IDH1*-mut samples were selected as training set.

The probability of class membership was transformed into a color code and plotted for each sample.

Statistical analysis

Statistical analyses were performed with Prism 6.0 (Graph Pad Software).

Results

SvGp12, U87-MG, and the primary glioblastoma cell line HT7606 were transduced with either *IDH1*-wt or *IDH1*-mut. The expression of *IDH1*-wt or $IDH1^{R132H}$ protein was confirmed using Western blot analysis (Supplementary Fig. S1). IR spectra were obtained from three independent preparations for each cell line.

Figure 1 shows the mean spectra of the three cell lines expressing either *IDH1*-wt or *IDH1*-mut. They display the same overall spectral pattern of bands that is a general feature of cells and tissue (dotted lines, band assignment; see Table 1). The spectra are dominated by the bands of amide II and amide I at 1550 and 1650 cm^{-1}, respectively. The spectral region of 950 to 1200 cm^{-1} results from the complex overlap of multiple molecular vibration bands of carbohydrates and nucleic acids. In this region, a cell line–specific spectral shape was observed (arrows in Fig. 1). For instance, U87-MG exhibits a small band at 1153 cm^{-1}, whereas HT7607 and SvGp12 show bands at 1173 cm^{-1}. Those characteristic spectral features of the cell lines were likewise found in *IDH1*-wt or *IDH*-mut–expressing cells.

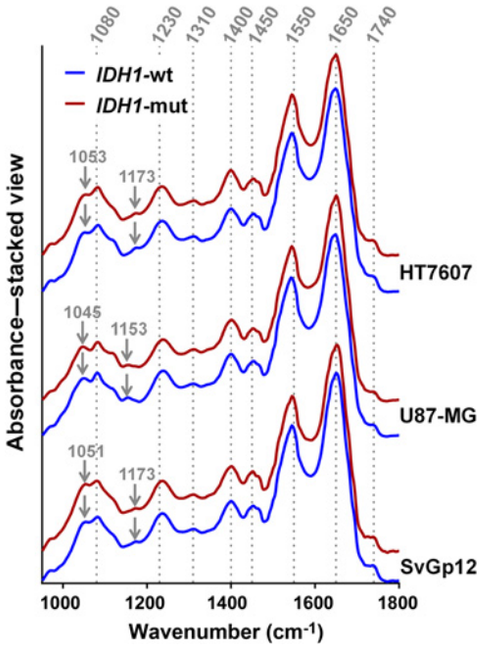

Figure 1.
IR spectra of cell lines expressing *IDH1*-wt or *IDH1*-mut. Mean transmission IR spectra are shown for HT7607, U87-MG, and SvGp12 ($n = 3$). Dotted lines, main bands; arrows, bands that exhibit shifts among the cell lines.

To identify a potential spectral marker for *IDH1* mutation, the IR spectra of the different cell lines were merged and grouped according to the *IDH1* mutation status. Figure 2A shows the mean IR spectra with SD for *IDH1*-wt cell lines and *IDH1*-mut cell lines.

At first glance, the IR spectra look related. Spectral differences become recognizable and are clearly separable in the difference spectrum (Fig. 2B, black spectrum). The spectral regions at 1000 to 1100, 1300 to 1430, and 1560 to 1610 cm^{-1} are more intense in *IDH1*-mut cell lines (i.e., regions where the difference spectrum is positive), whereas the band intensities in the regions at 1500 to 1545, 1625 to 1650, and 1690 to 1730 cm^{-1} are lower compared with the spectra of *IDH1*-wt cells. The comparison with the IR spectra of 2HG (Fig. 2B, gray spectrum), which is elevated in the case of *IDH1*-mut in human tumors and engineered cell lines (6, 28), indicated higher band intensities in the spectra of *IDH1*-mut cells at similar band positions (dashed lines). This might suggest that those bands reflect the increase of 2HG in the *IDH1*-mut cell lines. In addition, further spectral differences were observed (Fig. 2B, black arrows). The positive band at 1050 cm^{-1} is assigned to C-O stretching coupled with C-O bending of C-OH

Published OnlineFirst December 19, 2017; DOI: 10.1158/1078-0432.CCR-17-1795

Table 1. Main IR bands of cell lines and tissue. The corresponding molecular vibration and assigned tissue constituents are stated according to ref. 29

Spectral position	Molecular vibration	Tissue component
950–1200 cm^{-1} e.g.,	Multiple	DNA, RNA, carbohydrates, phospholipids
970 cm^{-1}	ν (CC), ν (PO_4^-)	DNA, RNA, phospholipids
1050 cm^{-1}	ν(CO), ν (PO_4^-)$_{sym}$	Carbohydrates, DNA, RNA
1080 cm^{-1}	ν(PO_2^-)$_{sym}$	Phospholipids, DNA, RNA
1120 cm^{-1}	ν(CO)	Ribose, RNA
1150 cm^{-1}	ν(CO)	Carbohydrates
1230 cm^{-1}	ν(PO_2^-)$_{asym}$	Phospholipids, DNA, RNA
1310 cm^{-1}	Amide III	Proteins
1340 cm^{-1}	δ(CH_2)	Proteins, lipids
1400 cm^{-1}	ν(COO^{2-})	Lipids
1450 cm^{-1}	δ(CH_3)	Proteins, lipids
1550 cm^{-1}	Amide II	Proteins
1650 cm^{-1}	Amide I	Proteins
1740 cm^{-1}	ν(C=O)	Lipids

Abbreviations: δ, deformation; ν, stretching; asym, antisymmetric; sym, symmetric.

groups and might indicate elevated carbohydrates, whereas the negative bands in the difference spectrum in the region around 1740 cm^{-1} are assigned to C=O stretching and might point to decreased lipid content in *IDH1*-mut cell lines. Moreover, bands assigned to vibrations of functional groups in proteins at 1522 and 1641 cm^{-1} suggest an altered protein profile (29).

The difference spectrum indicated that FT-IR spectroscopy is sensitive to metabolic changes induced by the *IDH1* mutation. Therefore, we tested whether *IDH1*-mut and *IDH1*-wt cell spectra can be mathematically discriminated. Sixteen positions of the spectra were selected, either corresponding to bands of the 2HG spectrum or to features in the difference spectrum. The following positions were chosen: (i) the band positions that were consistent with bands of 2HG (1072, 1174, 1203, 1311, 1344, 1416, 1450, 1568, and 1589 cm^{-1}; dashed lines in Fig. 2B); (ii) other bands of 2HG that were not identified in the difference spectrum (999, 1236, and 1267 cm^{-1}; gray arrows in Fig. 2B); and (iii) other maxima and minima of the difference spectrum (1043, 1522, 1641, and 1740 cm^{-1}; black arrows in Fig. 2B). On the basis of the absorbance at those spectral positions, the spectra were grouped in *IDH1*-wt and *IDH1*-mut with a correct rate of 92.2% by quadratic discriminant analysis (correct rate test set: 92.1%; reclassification rate training set: 92.6%). Figure 2C visualizes the result of the classification. Each lane represents one sample. The probability of class membership was calculated for all 256 spectra of one sample and is shown using color coding (see Supplementary Fig. S2). In all samples, the majority of the spectra were assigned to the correct class; a reliable discrimination was obtained for all cell lines. This shows that FT-IR spectroscopic data comprise the information about the *IDH1* mutation status, and that this information can be extracted in homogenous cell culture systems.

In the next step, we employed the technique to analyze cryosections of human brain tumor samples ($n = 34$; see Supplementary

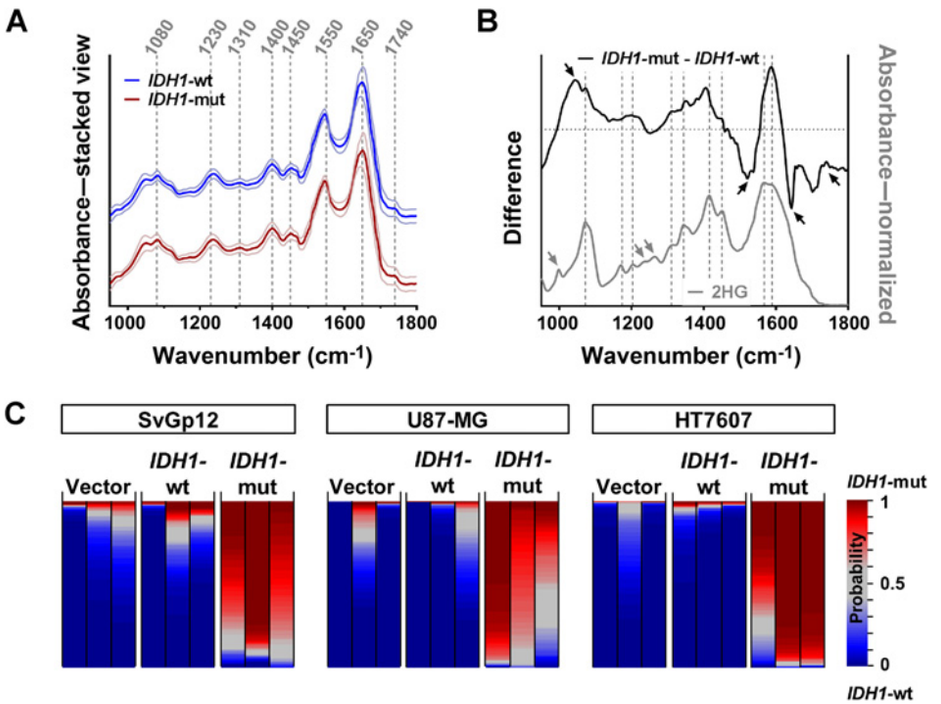

Figure 2.
Spectral differences of *IDH1*-wt and *IDH1*-mut cell lines. **A,** Mean transmission IR spectra ± SD, calculated merging SVG, U87, and HT7606 cell lines ($n = 3$ each). Dashed lines indicate the position of main bands. **B,** Difference spectra of *IDH1*-mut and *IDH1*-wt cell lines (black) and 2HG reference spectrum (gray). Spectral positions that were used for discrimination are indicated by dashed lines and arrows. **C,** Discrimination of *IDH1*-wt and *IDH1*-mut cell lines based on 22 spectral positions. Result of the quadratic discriminant analysis. For each sample, 256 spectra were analyzed, and the probability of class assignment was color coded and plotted in one lane.

Published OnlineFirst December 19, 2017; DOI: 10.1158/1078-0432.CCR-17-1795

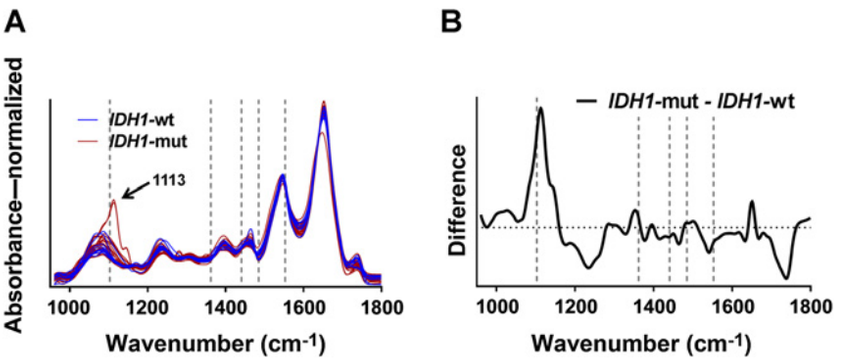

Figure 3.
Spectral differences of *IDH1*-wt and *IDH1*-mut human glioma samples. **A,** Mean transmission IR spectra of each tumor sample investigated ($n = 34$). **B,** Difference spectrum of *IDH1*-mut and *IDH1*-wt glioma. Spectral positions that were selected by the algorithm for classification are indicated by dashed gray lines.

Table S1). This allowed the selection of the measurement position on solid tumor according to reference pathology on consecutive sections. Many spectra were obtained for each sample to generate large datasets suitable for mathematical analysis. The mean spectra of all tumor samples are shown in Fig. 3A and display a high variability. This reflects the changes in tissue composition that vary among patients and among tumor types. As an example, two tumors exhibited an altered spectral shape at 1113 cm^{-1} that is assigned to $\nu(PO_4^-)_{sym}$ vibrations characteristic for acid phosphate of hydroxyapatite (Fig. 3A, arrow) and might indicate the presence of calcifications that are abundant in glioma (30). The corresponding difference spectrum (Fig. 3B) shows the strongest spectral features at 1113 cm^{-1}, representing the calcifications that were only found in *IDH1*-mut tumors. Furthermore, it indicated alterations in bands characteristic of nervous tissue (compare Table 1): Lower intensities around 1230 cm^{-1} indicate less phosphate groups and might be interpreted either as diminished DNA content or lower content of phospholipids in *IDH1*-mut tumor tissue. Similar cell numbers were found in *IDH1*-wt and *IDH1*-mut samples, suggesting similar DNA content (Supplementary Fig. S3). Therefore, alterations in the region around 1230 cm^{-1} rather represent decreased or altered phospholipids in *IDH1*-mut tumors. This is consistent with the lower intensity of the spectral band at 1740 cm^{-1} that is assigned to $\nu(C{=}O)$ and can be used for the assessment of overall lipid content in nervous tissue (Table 1).

The changes in the bands around 1550 and 1650 cm^{-1} might reflect variations in the protein profile. In addition, the more intense bands in the region 1005 to 1030 cm^{-1} suggest variations in carbohydrates. The interpretation of the band at 1352 cm^{-1}, which is increased in *IDH1*-mut tumor samples, is difficult. This band might reflect elevated levels of 2HG (band position at 1344 cm^{-1} in the reference spectrum of 2HG and at 1348 cm^{-1} in the difference spectrum of cell lines), but no other bands characteristic for 2HG were identified (compare Fig. 2B). Therefore, it might rather indicate an increase in proteins, especially collagen of the extracellular matrix (band of CH_2 wagging at 1340 cm^{-1}).

We used quadratic discriminant analysis to exploit the spectral information for the prediction of *IDH1* mutation status. Because of the high variability of human tissue samples, we employed an automatic selection routine to identify spectral regions suitable for classification. Five spectral regions were selected and are indicated in Fig. 3A and B as dashed gray lines (1103, 1362, 1441, 1485, and 1553 cm^{-1}). After using four samples of each group as training set, the algorithm provided a probability for the assignment to *IDH1*-wt or *IDH1*-mut class for each spectrum. This probability of class membership is shown in Fig. 4 for all samples. In 10 cases, all 256 spectra of the sample were assigned to the correct class. For the other cases, the sample's spectra were assigned to both groups. However, the majority (>70%) of spectra were assigned correctly to either *IDH1*-wt or *IDH1*-mut in 30 samples, retrieving the correct information about *IDH1* mutation status from the spectroscopic dataset (see Supplementary Table S1 for the result of the classification broken down by samples).

Four of the 34 tumor samples were not assigned to the correct class by the algorithm (indicated by asterisk in Fig. 4). However, no obvious spectral differences or indications for contamination were observed by looking at the misclassified spectra. It is important to state that spectra with distinct features such as calcifications

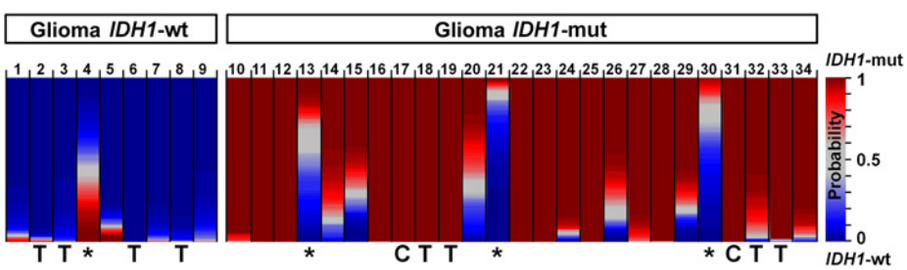

Figure 4.
Result of the classification of human glioma samples. Quadratic discriminant analysis was performed on five spectral positions (1103, 1362, 1441, 1485, and 1553 cm^{-1}). The probability of class assignment is plotted for each sample using a color code. The samples that were used as training set ("T") and samples that showed a strong band at 1113 cm^{-1} in the IR spectrum ("C") are indicated. Asterisks indicate misclassified samples.

Published OnlineFirst December 19, 2017; DOI: 10.1158/1078-0432.CCR-17-1795

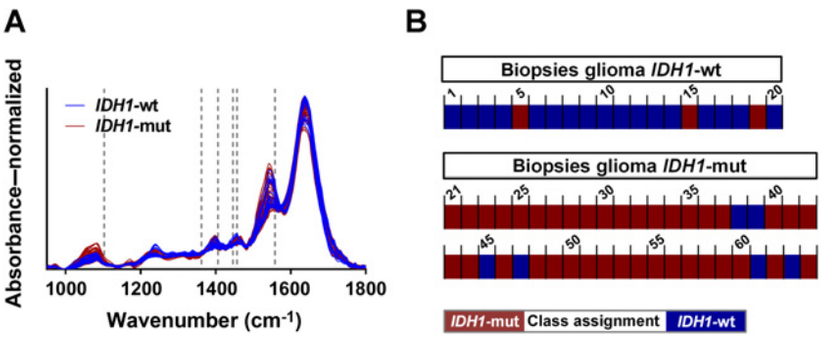

Figure 5.
Result of the classification of fresh human glioma biopsies. **A,** ATR IR spectra of 64 unprocessed, unfixed tumor samples. **B,** Quadratic discriminant analysis was performed on six spectral positions (1103, 1362, 1406, 1446, 1457, and 1558 cm^{-1}; indicated by dashed gray lines in **A**). The class assignment is plotted for each sample using a color code.

(band at 1113 cm^{-1}; compare Fig. 3A arrow) were correctly classified (labelled with "C" in Fig. 4).

We further tested our approach on fresh, unfixed bulk samples of human glioma ($n = 64$; Supplementary Table S2) to approximate a potential clinical application for intraoperative tissue analysis. Biopsies were directly obtained from the neurosurgeon and subjected to ATR FT-IR spectroscopy, a variant of infrared spectroscopy that allows the analysis of bulk samples. However, it has the limitation that the spectral signal of tissue is overlaid in some regions to the spectral signal originating from water (see Supplementary Fig. S4). Measurements were performed within minutes after removal (median, 6.5 minutes; range, 1–20 minutes) according to established protocols (26). The tissue spectra were obtained in approximately 1 minute and integrate the information from the region of sample that is in contact with the measurement crystal (area of $\sim 0.5 \times 0.5$ mm). The spectra of all samples are shown in Fig. 5A and confirm the high variability of human glioma similar to the spectra of tissue sections (compare Fig. 3A). Interestingly, the spectra with high band intensities in the region of around 1080 cm^{-1} fell into the group of *IDH1*-mut tumors. Quadratic discriminant analysis was performed on the basis of the spectral regions 1103, 1362, 1406, 1446, 1457, and 1558 cm^{-1} (dashed lines in Fig. 5A) and assigned 55 of the 64 spectra correctly to the *IDH1*-mut or *IDH1*-wt group (Fig. 5B; correct rate: 86%, correct rate test set: 82%, reclassification rate training set: 95%). Four of the nine misclassified samples were identified as infiltrating tumor, and three were obtained from recurrent glioma, whereas two misclassified samples did not have any specific histologic or clinical features.

Discussion

Here, we show for the first time that FT-IR spectroscopy of tissue samples provides information about a specific genetic alteration. We focused on *IDH1* mutation in brain tumors, as it is known to alter cell metabolism and therefore, constitutes an ideal target for vibrational spectroscopic techniques. FT-IR spectroscopy does not directly detect the missense mutation at the level of the DNA or the replacement of arginine at 132 of the IDH1 protein but rather addresses changes in the biochemistry of the cell that are the consequence of the *IDH1* mutation. The spectral changes might reflect both metabolic and epigenetics alterations (methylation of histones), which can be addressed by vibrational spectroscopy (31, 32).

The most prominent metabolic change in *IDH1*-mut tumor cells is the increased level of 2HG (6). Spectral features that might be consistent with 2HG increase were detected in the difference spectra of the *IDH1*-mut versus *IDH1*-wt cell lines. Glioma cell lines that were genetically modified to express IDH1-mut were shown to express high levels of 2HG (28, 33, 34). However, the increase of 2HG was not obvious in the difference spectrum of human glioma. It was either masked by overlapping contributions of other tissue constituents, or the difference in 2HG may be not evident when merging patients' datasets. The level of 2HG is highly variable among patients [4.50–31.56 μmol/g (6), up to 2,000 nmol/mg in secondary glioblastoma (10), 2.53 ± 0.75 μmol/g in glioma (35), ∼10–50 μg/mg protein (36)]. Furthermore, an overlap in 2HG levels in *IDH1*-wt and *IDH1*-mut glioma was shown (37), and some *IDH1*-mut tumor tissue might not even show detectable levels of 2HG (38). Therefore, metabolic changes other than production of 2HG account for the spectral differences observed in our study.

Similar spectral regions allowed the classification of *IDH1*-mut and *IDH1*-wt tumors in fresh samples or cryosections (compare dashed lines in Figs. 3A and 5A). Therefore, band assignment to functional groups might help to gain insight into the underlying biochemical differences. The band at 1103 cm^{-1} is assigned to C-O stretching vibrations and might indicate changes of carbohydrates. The bands at 1362 and 1441 (sections), 1446 (fresh tissue), and 1457 cm^{-1} (fresh tissue) can be related to CH_2 bending in fatty acids. The spectral position at 1406 (fresh tissue) and 1485 cm^{-1} (sections) can be assigned to COO^- symmetric stretching vibrations and to C-H deformation, respectively. Those can be likewise attributed to fatty acids and proteins. However, the spectral positions at 1558 (sections) and 1553 cm^{-1} (fresh tissue) are clearly related to amide II and, therefore, to proteins (29, 39). In combination with the analysis of the difference spectra, this underlines the importance of lipid- and protein-related spectral bands for recognition of *IDH1* mutation status in human glioma.

It is well-known that *IDH1* mutations cause global changes in cellular metabolism and signaling (40). The pathways that depend on normal IDH1 activity are impaired, levels of NAPDH are strongly reduced, and gene expression is altered by hypermethylation (3). In the current study, we assigned spectral changes to variations in (phospho-)lipid content and protein profile based on FT-IR spectroscopic datasets of both cell lines and human glioma. This is consistent with the changed phospholipid profile found in experimental and human glioma. In both models, *IDH1*-mut tumors displayed decreased levels of phosphoethanolamine and increased levels of glycerophosphocholine (41), and a significant decrease in phosphocholine was observed in *IDH1*-mut cell lines (28). Interestingly, increased band intensities at 1380, 1455, and 1465 cm^{-1} were found

Published OnlineFirst December 19, 2017; DOI: 10.1158/1078-0432.CCR-17-1795

in hypoxic glioma cells analyzed by IR spectroscopy and were interpreted as an altered lipid signal (39). *IDH1*-mut glioma are known to express higher levels of HIF-1α that is usually upregulated in hypoxic conditions (42).

IR spectroscopy does not allow the extraction of information on specific proteins if analyzing tissue samples. However, the data indicated a genotype-related altered protein profile. This is consistent with variations of amino acid levels in *IDH1*-mutated cell lines and tumor tissue that have been reported by others: *IDH1*-mutated cell lines showed elevated levels of glycine, serine, threonine, asparagine, phenylalanine, tyrosine, tryptophan, and methionine, whereas aspartate was decreased (40). Furthermore, n-acetylated amino acids were found to be reduced in *IDH1*-mut cells. Lower levels of amino acids (phenylalanine, glutamine, and glutamate) and amino acid derivate (n-acetyl-glutamate, n-acetyl-aspartate, and n-acetyl-histidine) were observed in human glioma (43). In contrast, *IDH1* mutation does not alter the levels of glycolytic or pentose phosphate pathway intermediates (28, 40, 43).

Comprehensive interpretation and understanding of the entire molecular changes that are pictured in the IR spectra of *IDH1*-mut versus *IDH1*-wt cells and tumors were not possible in the frame of this study. This might be in part due to the fact that bands assigned to certain molecular vibrations are overlapping. Related to this intrinsic biochemical unspecificity, underlying causes of sample misclassification (four cryosections and nine fresh biopsies) remain unclear. Analysis of misclassified spectra did not provide conclusive results due to tumor heterogeneity that was likewise reflected in high interpatient variability of the IR spectra. However, the finding that infiltrative tumors were among the misclassified fresh biopsies might indicate a limitation of the technique and/or of the classification strategy. Further research is needed for evaluation of vibrational spectroscopy for detection of *IDH1* mutation in the infiltration zone.

In the current study, spectroscopic data were shown to comprise the information about the *IDH1* mutation status of human glioma that constitutes a prognostic factor. Furthermore, determination of the *IDH1* mutation is essential for current glioma grading according to the World Health Organization (WHO; ref. 44) and might influence therapeutic decisions or frequency of screening after glioma resection.

We used FT-IR spectroscopy on cryosections of frozen tissue samples to validate the method. Furthermore, ATR FT-IR spectroscopy of fresh, unfixed biopsies of human glioma confirmed our findings despite the disturbance due to the spectral contributions of water. As an alternative vibrational spectroscopic technique, which compared with IR spectroscopy is relatively insensitive to water content inside the tissue, Raman spectroscopy can be employed as well. Furthermore, fiber-based technical solutions might be applied to obtain spectroscopic information even *in situ*, before removing suspicious tissue, as recently shown using Raman spectroscopy for analysis of human glioma (17). In that study, diagnostic information was provided within 0.2 seconds using a hand-held Raman probe in patients with glioma.

Therefore, an intraoperative assessment of the *IDH1* mutation status in glioma by vibrational spectroscopy is technically feasible and manageable in the clinical context. Perspectively, this opens the possibility to analyze brain tumors at multiple positions during regular resection and to obtain intraoperative diagnostic information about *IDH1* mutations within seconds. From a clinical perspective, a rapid assessment of the *IDH* mutation status facilitates intraoperative neurosurgical decisions. It helps distinguish tumor from nonneoplastic lesions, especially in limited tissue, and therefore, decreases the risk from additional samplings in stereotactic biopsies (13). Furthermore, unlike primary glioblastoma, *IDH1*-mutant gliomas benefit from complete resection of enhancing and nonenhancing disease (45).

On the basis of the current findings, we expect that other clinically relevant mutations and (epi)genetic changes that influence metabolics or tissue composition are amenable to vibrational spectroscopy. Besides *IDH1* mutation, other diagnostic, prognostic, and predictive molecular markers of brain tumors like α-thalassemia/mental retardation syndrome X-linked (ATRX) gene mutation, 1p/19q codeletion, and telomerase reverse transcriptase (TERT) promoter mutation or O6-methylguanine-DNA methyltransferase (MGMT) promoter methylation are of paramount clinical importance and guide treatment decisions (46).

In conclusion, optical spectroscopy constitutes a translational approach for brain tumor analysis, although with the limitation that the threshold of tumor infiltration required to produce a spectral difference remains unknown. In perspective, fast optical biopsies *in situ* might allow the adaptation of resection strategy and the immediate application of local therapies. Personalized treatment regimens could be started early in the therapeutic process based on the spectral fingerprint of the patient's tumor.

Disclosure of Potential Conflicts of Interest

No potential conflicts of interest were disclosed.

Authors' Contributions

Conception and design: O. Uckermann, T.A. Juratli, E. Koch, M. Kirsch
Development of methodology: O. Uckermann, R. Galli, M. Conde, K. Geiger, G. Steiner
Acquisition of data (provided animals, acquired and managed patients, provided facilities, etc.): O. Uckermann, T.A. Juratli, M. Conde, R. Wiedemuth, D. Krex, K. Geiger, M. Kirsch
Analysis and interpretation of data (e.g., statistical analysis, biostatistics, computational analysis): O. Uckermann, T.A. Juratli, R. Galli, M. Conde, K. Geiger, G. Steiner, M. Kirsch
Writing, review, and/or revision of the manuscript: O. Uckermann, T.A. Juratli, R. Galli, D. Krex, A. Temme, G. Schackert, E. Koch, G. Steiner, M. Kirsch
Administrative, technical, or material support (i.e., reporting or organizing data, constructing databases): O. Uckermann, A. Temme, G. Schackert, M. Kirsch
Study supervision: M. Kirsch
Other (neuropathologic evaluation): K. Geiger

Acknowledgments

Financial support was received from Bundesministerium für Bildung und Forschung (BMBF "EndoCARS" 13N13807; to M. Kirsch and E. Koch, and "MediCARS" 13N10777; to G. Schackert, M. Kirsch, and E. Koch), Medical Faculty of TU Dresden (Habilitationsförderung für Frauen; to O. Uckermann), and European Union and Free State of Saxony (EU-ESF GlioMath-DD; to A. Temme). The authors thank Elke Leipnitz for excellent technical assistance and Dr. Barbara Klink, Institut für Klinische Genetik, Medizinische Fakultät Carl Gustav Carus, TU Dresden, Dresden, Germany, for providing the original SvGp12 cell line.

The costs of publication of this article were defrayed in part by the payment of page charges. This article must therefore be hereby marked *advertisement* in accordance with 18 U.S.C. Section 1734 solely to indicate this fact.

Received June 27, 2017; revised October 16, 2017; accepted December 14, 2017; published first December 19, 2017.

Published OnlineFirst December 19, 2017; DOI: 10.1158/1078-0432.CCR-17-1795

References

1. Hartmann C, Meyer J, Balss J, Capper D, Mueller W, Christians A, et al. Type and frequency of IDH1 and IDH2 mutations are related to astrocytic and oligodendroglial differentiation and age: a study of 1,010 diffuse gliomas. Acta Neuropathol 2009;118:469–74.
2. Juratli TA, Kirsch M, Robel K, Soucek S, Geiger K, von KR, et al. IDH mutations as an early and consistent marker in low-grade astrocytomas WHO grade II and their consecutive secondary high-grade gliomas. J Neurooncol 2012;108:403–10.
3. Waitkus MS, Diplas BH, Yan H. Isocitrate dehydrogenase mutations in gliomas. Neuro Oncol 2016;18:16–26.
4. Sanson M, Marie Y, Paris S, Idbaih A, Laffaire J, Ducray F, et al. Isocitrate dehydrogenase 1 codon 132 mutation is an important prognostic biomarker in gliomas. J Clin Oncol 2009;27:4150–4.
5. Louis DN, Perry A, Burger P, Ellison DW, Reifenberger G, von DA, et al. International Society of Neuropathology–Haarlem consensus guidelines for nervous system tumor classification and grading. Brain Pathol 2014; 24:429–35.
6. Dang L, White DW, Gross S, Bennett BD, Bittinger MA, Driggers EM, et al. Cancer-associated IDH1 mutations produce 2-hydroxyglutarate. Nature 2009;462:739–44.
7. Prensner JR, Chinnaiyan AM. Metabolism unhinged: IDH mutations in cancer. Nat Med 2011;17:291–3.
8. Cahill DP, Sloan AE, Nahed BV, Aldape KD, Louis DN, Ryken TC, et al. The role of neuropathology in the management of patients with diffuse low grade glioma: a systematic review and evidence-based clinical practice guideline. J Neurooncol 2015;125:531–49.
9. Preusser M, Wohrer A, Stary S, Hoftberger R, Streubel B, Hainfellner JA. Value and limitations of immunohistochemistry and gene sequencing for detection of the IDH1-R132H mutation in diffuse glioma biopsy specimens. J Neuropathol Exp Neurol 2011;70:715–23.
10. Choi C, Ganji SK, DeBerardinis RJ, Hatanpaa KJ, Rakheja D, Kovacs Z, et al. 2-hydroxyglutarate detection by magnetic resonance spectroscopy in IDH-mutated patients with gliomas. Nat Med 2012;18:624–9.
11. Pope WB, Prins RM, Albert TM, Nagarajan R, Yen KE, Bittinger MA, et al. Non-invasive detection of 2-hydroxyglutarate and other metabolites in IDH1 mutant glioma patients using magnetic resonance spectroscopy. J Neurooncol 2012;107:197–205.
12. Dunn GP, Andronesi OC, Cahill DP. From genomics to the clinic: biological and translational insights of mutant IDH1/2 in glioma. Neurosurg Focus 2013;34:E2.
13. Shankar GM, Francis JM, Rinne ML, Ramkissoon SH, Huang FW, Venteicher AS, et al. Rapid intraoperative molecular characterization of glioma. JAMA Oncol 2015;1:662–7.
14. Broadbent B, Tseng J, Kast R, Noh T, Brusatori M, Kalkanis SN, et al. Shining light on neurosurgery diagnostics using Raman spectroscopy. J Neurooncol 2016;130:1–9.
15. Hollon T, Lewis S, Freudiger CW, Sunney Xie X, Orringer DA. Improving the accuracy of brain tumor surgery via Raman-based technology. Neurosurg Focus 2016;40:E9.
16. Diem M, Mazur A, Lenau K, Schubert J, Bird B, Miljkovic M, et al. Molecular pathology via IR and Raman spectral imaging. J Biophotonics 2013;6:855–86.
17. Jermyn M, Mok K, Mercier J, Desroches J, Pichette J, Saint-Arnaud K, et al. Intraoperative brain cancer detection with Raman spectroscopy in humans. Sci Transl Med 2015;7:274ra19.
18. Orringer DA, Pandian B, Niknafs YS, Hollon TC, Boyle J, Lewis S, et al. Rapid intraoperative histology of unprocessed surgical specimens via fibre-laser-based stimulated Raman scattering microscopy. Nat Biomed Eng 2017;1:0027.
19. Kalkanis SN, Kast RE, Rosenblum ML, Mikkelsen T, Yurgelevic SM, Nelson KM, et al. Raman spectroscopy to distinguish grey matter, necrosis, and glioblastoma multiforme in frozen tissue sections. J Neurooncol 2014;116:477–85.
20. Krafft C, Thummler K, Sobottka SB, Schackert G, Salzer R. Classification of malignant gliomas by infrared spectroscopy and linear discriminant analysis. Biopolymers 2006;82:301–5.
21. Krafft C, Shapoval L, Sobottka SB, Schackert G, Salzer R. Identification of primary tumors of brain metastases by infrared spectroscopic imaging and linear discriminant analysis. Technol Cancer Res Treat 2006; 5:291–8.
22. Steiner G, Mackenroth L, Geiger KD, Stelling A, Pinzer T, Uckermann O, et al. Label-free differentiation of human pituitary adenomas by FT-IR spectroscopic imaging. Anal Bioanal Chem 2012;403:727–35.
23. Hendruschk S, Wiedemuth R, Aigner A, Topfer K, Cartellieri M, Martin D, et al. RNA interference targeting survivin exerts antitumoral effects in vitro and in established glioma xenografts in vivo. Neuro Oncol 2011; 13:1074–89.
24. Muller N, Michen S, Tietze S, Topfer K, Schulte A, Lamszus K, et al. Engineering NK cells modified with an EGFRvIII-specific chimeric antigen receptor to overexpress CXCR4 improves immunotherapy of CXCL12/SDF-1alpha-secreting glioblastoma. J Immunother 2015;38: 197–210.
25. Tamosaityte S, Galli R, Uckermann O, Sitoci-Ficici KH, Later R, Beiermeister R, et al. Biochemical monitoring of spinal cord injury by FT-IR spectroscopy–effects of therapeutic alginate implant in rat models. PLoS One 2015;10:e0142660.
26. Stelling AL, Toher D, Uckermann O, Tavkin J, Leipnitz E, Schweizer J, et al. Infrared spectroscopic studies of cells and tissues: triple helix proteins as a potential biomarker for tumors. PLoS One 2013;8:e58332.
27. Steiner G, Kuchler S, Hermann A, Koch E, Salzer R, Schackert G, et al. Rapid and label-free classification of human glioma cells by infrared spectroscopic imaging. Cytometry A 2008;73A:1158–64.
28. Izquierdo-Garcia JL, Viswanath P, Eriksson P, Chaumeil MM, Pieper RO, Phillips JJ, et al. Metabolic reprogramming in mutant IDH1 glioma cells. PLoS One 2015;10.
29. Movasaghi Z, Rehman S, ur Rehman D. Fourier transform infrared (FTIR) spectroscopy of biological tissues. Appl Spectrosc Rev 2008;43:134–79.
30. Ramonet D, de Yebra L, Fredriksson K, Bernal F, Ribalta T, Mahy N. Similar calcification process in acute and chronic human brain pathologies. J Neurosci Res 2006;83:147–56.
31. Dunn WB, Bailey NJC, Johnson HE. Measuring the metabolome: current analytical technologies. Analyst 2005;130:606–25.
32. Kelly JG, Najand GM, Martin FL. Characterisation of DNA methylation status using spectroscopy (mid-IR versus Raman) with multivariate analysis. J Biophotonics 2011;4:345–54.
33. Bralten LB, Kloosterhof NK, Balvers R, Sacchetti A, Lapre L, Lamfers M, et al. IDH1 R132H decreases proliferation of glioma cell lines *in vitro* and *in vivo*. Ann Neurol 2011;69:455–63.
34. Wen H, Cho HR, Yun T, Kim H, Park CK, Lee SH, et al. Metabolomic comparison between cells over-expressing isocitrate dehydrogenase 1 and 2 mutants and the effects of an inhibitor on the metabolism. J Neurochem 2015;132:183–93.
35. Emir UE, Larkin SJ, de Pennington N, Voets N, Plaha P, Stacey R, et al. Noninvasive quantification of 2-hydroxyglutarate in human gliomas with IDH1 and IDH2 mutations. Cancer Res 2016;76:43–9.
36. Jin G, Reitman ZJ, Spasojevic I, Batinic-Haberle I, Yang J, Schmidt-Kittler O, et al. 2-Hydroxyglutarate production, but not dominant negative function, is conferred by glioma-derived NADP+-dependent isocitrate dehydrogenase mutations. PLoS One 2011;6:e16812.
37. Juratli TA, Peitzsch M, Geiger K, Schackert G, Eisenhofer G, Krex D. Accumulation of 2-hydroxyglutarate is not a biomarker for malignant progression in IDH-mutated low-grade gliomas. Neuro Oncol 2013; 15:682–90.
38. Kalinina J, Carroll A, Wang L, Yu Q, Mancheno DE, Wu S, et al. Detection of oncometabolite 2-hydroxyglutarate by magnetic resonance analysis as a biomarker of IDH1/2 mutations in glioma. J Mol Med 2012;90:1161–71.
39. Sandt C, Nadaradjane C, Richards R, Dumas P, See V. Use of infrared microspectroscopy to elucidate a specific chemical signature associated with hypoxia levels found in glioblastoma. Analyst 2016;141: 870–83.
40. Reitman ZJ, Jin GL, Karoly ED, Spasojevic I, Yang JA, Kinzler KW, et al. Profiling the effects of isocitrate dehydrogenase 1 and 2 mutations on the cellular metabolome. Proc Natl Acad Sci U S A 2011;108:3270–5.
41. Esmaeili M, Hamans BC, Navis AC, van Horssen R, Bathen TF, Gribbestad IS, et al. IDH1 R132H mutation generates a distinct phospholipid metabolite profile in glioma. Cancer Res 2014;74:4898–907.
42. Zhao S, Lin Y, Xu W, Jiang W, Zha Z, Wang P, et al. Glioma-derived mutations in IDH1 dominantly inhibit IDH1 catalytic activity and induce HIF-1alpha. Science 2009;324:261–5.

Published OnlineFirst December 19, 2017; DOI: 10.1158/1078-0432.CCR-17-1795

43. Ohka F, Ito M, Ranjit M, Senga T, Motomura A, Motomura K, et al. Quantitative metabolome analysis profiles activation of glutaminolysis in glioma with IDH1 mutation. Tumour Biol 2014;35:5911–20.
44. Louis DN, Perry A, Reifenberger G, von DA, Figarella-Branger D, Cavenee WK, et al. The 2016 world health organization classification of tumors of the central nervous system: a summary. Acta Neuropathol 2016;131: 803–20.
45. Beiko J, Suki D, Hess KR, Fox BD, Cheung V, Cabral M, et al. IDH1 mutant malignant astrocytomas are more amenable to surgical resection and have a survival benefit associated with maximal surgical resection. Neuro Oncol 2014;16:81–91.
46. Masui K, Mischel PS, Reifenberger G. Molecular classification of gliomas. In: Berger MS, Weller M, editors. Handbook of clinical neurology: gliomas. vol. 134. Amsterdam (Netherlands): Elsevier; 2016. p. 97–120.

Published OnlineFirst December 19, 2017; DOI: 10.1158/1078-0432.CCR-17-1795

Clinical Cancer Research

Optical Analysis of Glioma: Fourier-Transform Infrared Spectroscopy Reveals the *IDH1* Mutation Status

Ortrud Uckermann, Tareq A. Juratli, Roberta Galli, et al.

Clin Cancer Res 2018;24:2530-2538. Published OnlineFirst December 19, 2017.